Supplement of Earth Syst. Sci. Data, 13, 3791–3818, 2021
https://doi.org/10.5194/essd-13-3791-2021-supplement

Open Access Earth System Science Data

Supplement of

Mass balances of Yala and Rikha Samba glaciers, Nepal, from 2000 to 2017

Dorothea Stumm et al.

Correspondence to: Dorothea Stumm (stummd@gmail.com)

S1 A brief description of summer-accumulation-type glaciers and related mass-balance measurements

On summer-accumulation-type glaciers the main ablation and accumulation season coincide in the monsoon season (Fig. S1.; Ageta and Higuchi, 1984). Summer-accumulation-type glaciers with a balanced mass budget experience the majority of snowfall on high elevations during the monsoon season. In autumn and winter, snow accumulation is usually low but depends on the interannually very variable precipitation events as a result of westerly disturbances and cyclones (Fujita et al., 1997). Melt starts in the pre-monsoon season and continues throughout the monsoon season. In autumn and winter melt is minimal.

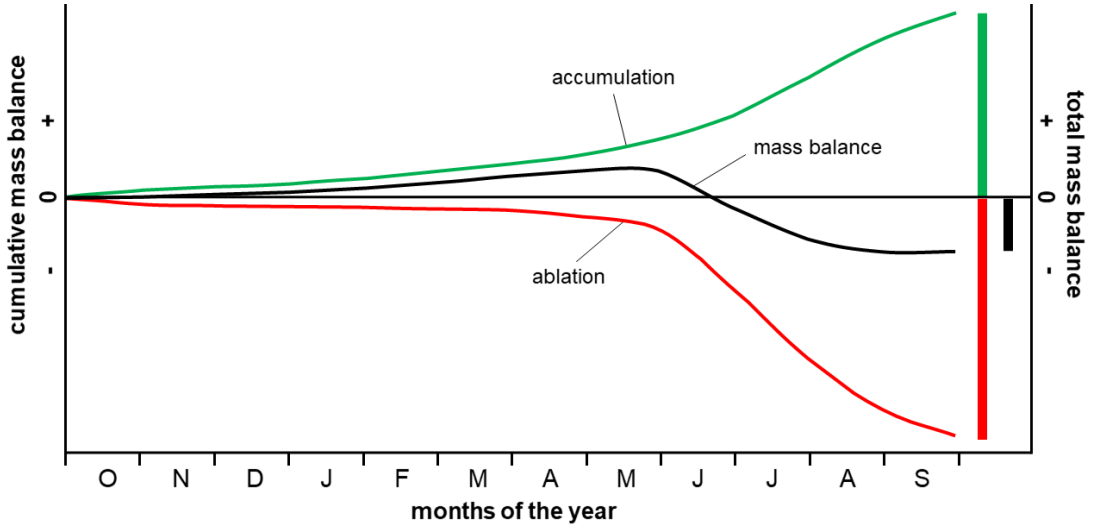

Figure S1: An example of the cumulative ablation, accumulation and mass balance of a summer-accumulation-type glacier over the course of a mass-balance year.

During monsoon, the altitude of the transient snowline on the glacier fluctuates and is very sensitive to the temperature, especially during precipitation events. At the end of the monsoon season the altitude of the snowline depends on both the preceding temperatures and precipitation. Consequently, on summer-accumulation-type glaciers the snowline at the end of the monsoon season does not necessarily coincide with the approximate equilibrium line and is not a reliable proxy for the equilibrium-line altitude (ELA).

Ablation on glacier ice is usually measured with stakes, and accumulation with snow pits including snow depth, density and profile measurements (Kaser et al., 2003). In case of accumulation measurements snow cores are practical and more feasible than snow pits if the snow is hard and metamorphized from melt and refreezing processes during monsoon. Snow profiles are used to identify ice layers and characteristics snow layers. When snow is probed, it is important to take multiple measurements and to consider ice layers found in snow profiles to assess the representativeness of the measurements.

Measuring and analysing the point mass balance in the ablation area tends to be straightforward. In the ablation area, the ice is possibly covered with snow. The ablation on the ice can be measured with stakes. If snow is present, the snow accumulation can be measured with snow pits. For the point mass-balance calculation, the ablation and accumulation are added up.

Measuring the mass balance in the accumulation area can be difficult. New snow from the current mass-balance year is lying on top of snow and firn layers from previous mass-balance years. An annual dust layer separating new snow from snow from previous mass-balance years is often absent or unreliable. The reasons are the moist

monsoon months when little dust is in the atmosphere to be deposited on the snow, and fresh snowfall preventing the accumulation of a distinct dust layer. To mark the current glacier surface in the field, an unsolvable powder (e.g. sawdust or blue carpenter chalk) is spread on the surface, covered by snow to protect from ablation. The location is marked with a stake.

The challenges of mass-balance measurements in the accumulation area depend to a large degree on the timing of ablation and accumulation. If the cumulative accumulation is always larger than the cumulative ablation during the entire measurement period, the mass balance can be measured with snow pits or snow cores, provided the previous year's glacier surface can be identified (Scenario 1 in Fig. S2). This is the case in large parts of accumulation areas of glaciers with a large elevation range in the accumulation area.

Measurements are challenging if the cumulative ablation exceeds the cumulative accumulation during parts of the monitoring period (Scenarios 2 and 3 in Fig. S2). This can be the case in areas close to the equilibrium line where warm temperatures cause increased melt, or at locations where the glacier is exposed to ablation by wind drift. On one hand, the ablation cannot be reliably measured with stakes installed in an unstable firn underground that compacts over time and may push or pull the stake up or down. On the other hand, accumulation can be difficult to be quantified because ablation removed the marked reference glacier surface. The uncertainty of mass-balance measurements is larger in such areas than in ablation areas, and an overestimated positive mass balance is likely.

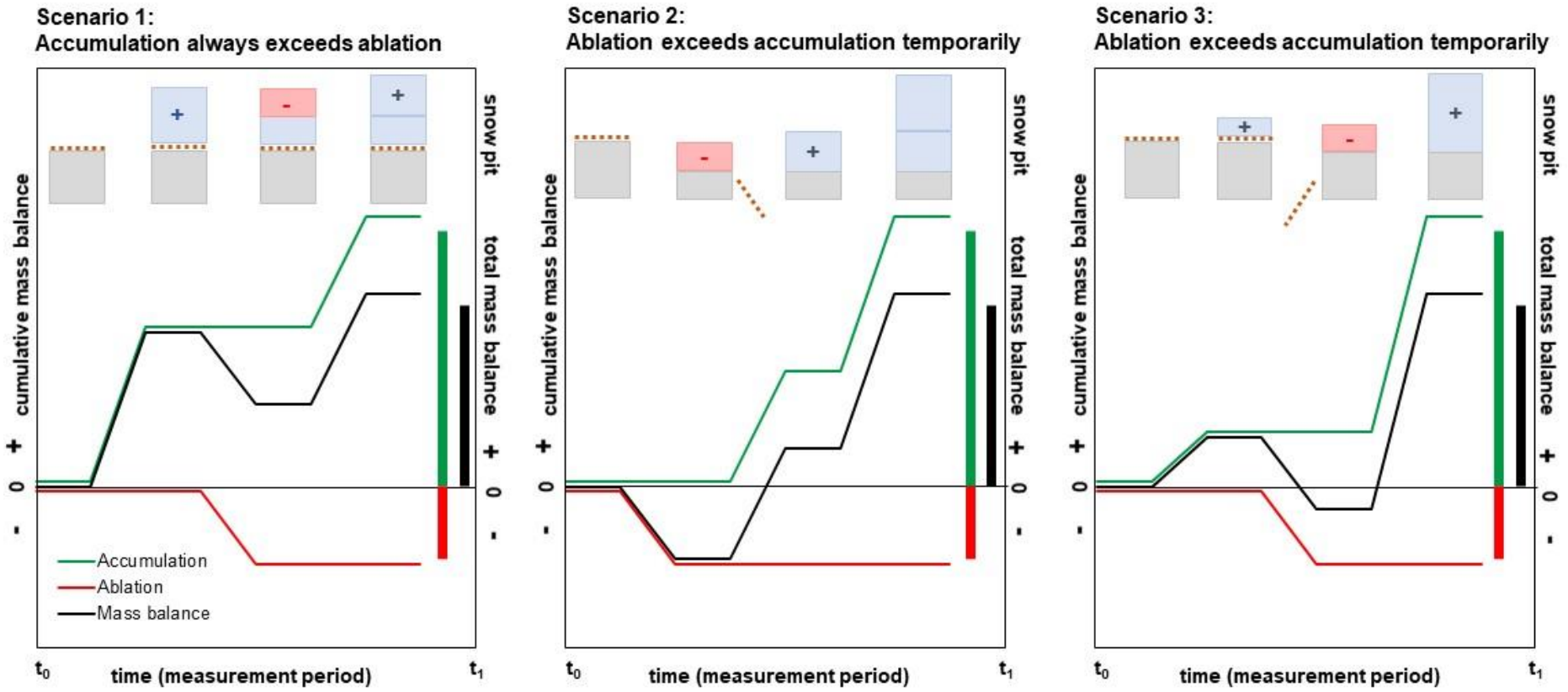

Figure S2: Three schematic scenarios of the evolvement of accumulation, ablation and mass balance in parts of an accumulation area during one measurement season (bottom graphs), and the impact on the snow and firn layers in a snow pit (top sketches). In the sketch, snow and firn from the previous measurement period are marked grey and the layer marking the surface artificially is the dashed brown line. Snow accumulation and snow ablation are marked blue and red, respectively. In all three scenarios the total amount of accumulation, ablation and mass balance are the same. But in scenarios two and three the temporarily exceeding ablation removes the marked layer on the reference surface, making the measurement and analysis challenging.

S2 Differential GNSS measurements, evaluated maps and used satellite products

Table S1: Differential GNSS data collected and its usage for Yala and Rikha Samba glaciers. The accuracy of the dGNSS measurements mainly depends on access and measurement duration.

Yala Glacier			
Date	**Product**	**Usage**	**Horizontal accuracy**
8.5.2012	differential GNSS (Magellan, ProMark-3)	stake locations	±0.3 m
		velocity	±0.4 m
		surface profiles	±0.4 m
3.11.2012	Garmin GPSmap 60CSx	terminus	<10 m
6.5.2014	differential GNSS (Topcon)	stake locations	±0.3 m
5.5.2014		velocity	±0.4 m
5.5.2014		terminus	±1-2 m
8.5.2016	differential GNSS (Topcon)	terminus	±1-3 m
25.4.2017	differential GNSS (Topcon)	stake locations	±0.3 m
Rikha Samba Glacier			
30.9.2013	differential GNSS (Topcon)	terminus	±1-2 m
3.10.2013		stake locations	±0.3 m
3-7.10.2015	differential GNSS (Topcon)	stake locations	±0.3 m

Table S2: Maps and data sources evaluated for glacier surface and area change analysis for Yala Glacier. The estimated accuracy of topographic maps is based on the map scale (e.g. in 1:50,000 map = 50 m). The maps known in Nepal as Schneider maps are labelled as "Alpenvereinskarte" (Alpine Club Map), and named after "Schneider's method" for the aerial photograph interpretation. The map was published within the framework of the Alpenvereinskartographie by the Austrian Alpine Club (Oesterreichischer Alpenverein) in 1990.

Publishing year	Name	Map ID	Scale	Accuracy	Map source	Reference	Usage
1965	Survey of India Map	71 H/12	1:63,360	±48–63 m (estimated)	Aerial photos 1957/58, field surveys; scanned map	Survey of India	Problems with transformation and scale, not used
1990	Schneider Map / Austrian Alpine Club Map	Langthang Himal Ost 0/11	1:50,000	±40–50 m (estimated)	Aerial photos 1970/71, field surveys; scanned map	Kostka et al., 1990	Transformation problem, not used
1984	GEN map	Yala Glacier	1:5,000	XY: ±4–5 m Z: ±0.45 m (estimated), terminus ~2-3 m	Ground photogrammetry, field surveys 1981; scanned map	Yokoyama, 1984, provided by K. Fujita	Terminus; for area and surface change not used due to transformation problems
1995	Nepal Topographic Map/ Finn Map	2885-15	1:50,000	>10 m (estimated)	Aerial photo 1992, field surveys; vector map		Transformation problems, not used
2014	ICIMOD glacier inventory	Yala Glacier	~1:50,000	±30 m, terminus and outline ±15 m	Landsat 7 ETM+, vector map	Bajracharya et al. 2014	Terminus Glacier outlines modified

Table S3: Overview of used remote sensing data for Yala and Rikha Samba glaciers.

Year	Sensor	Scene ID	Geometric resolution	Usage
Yala Glacier				
23.11.1974	Hexagon KH-9	DZB1209-500101L006001 DZB1209-500101L007001	±7.6 m (varying from 6 – 9 m)	Frontal variations
2000	SRTM3	2128125658	±90 m	DEM (SRTM-3) GCP generation (z)
Feb 2000	Landsat 7 ETM+		±30 m	Frontal variations Glacier outline
15.1.2012	GeoEye-1 (stereo)	20120115050057616030 31609567	±0.5 m (Pan) ±1.65 m (Multispectral)	DEM (DEM2012) Orthoimage for glacier outline
2013	Landsat-8	LC81410402013322LGN0 0	±15 m (Pan) ±30 m (Multispectral)	GCP generation (x,y)
Rikha Samba Glacier				
7.3.1989	Landsat MSS 4		±60 m	Terminus
2000	SRTM1	SRTM_53_07 SRTM_54_07	±30 m	DEM, voids filled with SRTM3 data
29.9.2001	Landsat 7 ETM+		±30 m	Terminus
7.2.2006	Landsat 5 TM		±30 m	Terminus
25.4.2010 27.4.2010	RapidEye	4452325_2010-04-25 4452325_2010-04-27	±5 m	Outline
5.2.2011	Landsat 5 TM		±30 m	Terminus

S3 Mass balances and uncertainties for elevation bands at Yala and Rikha Samba glaciers

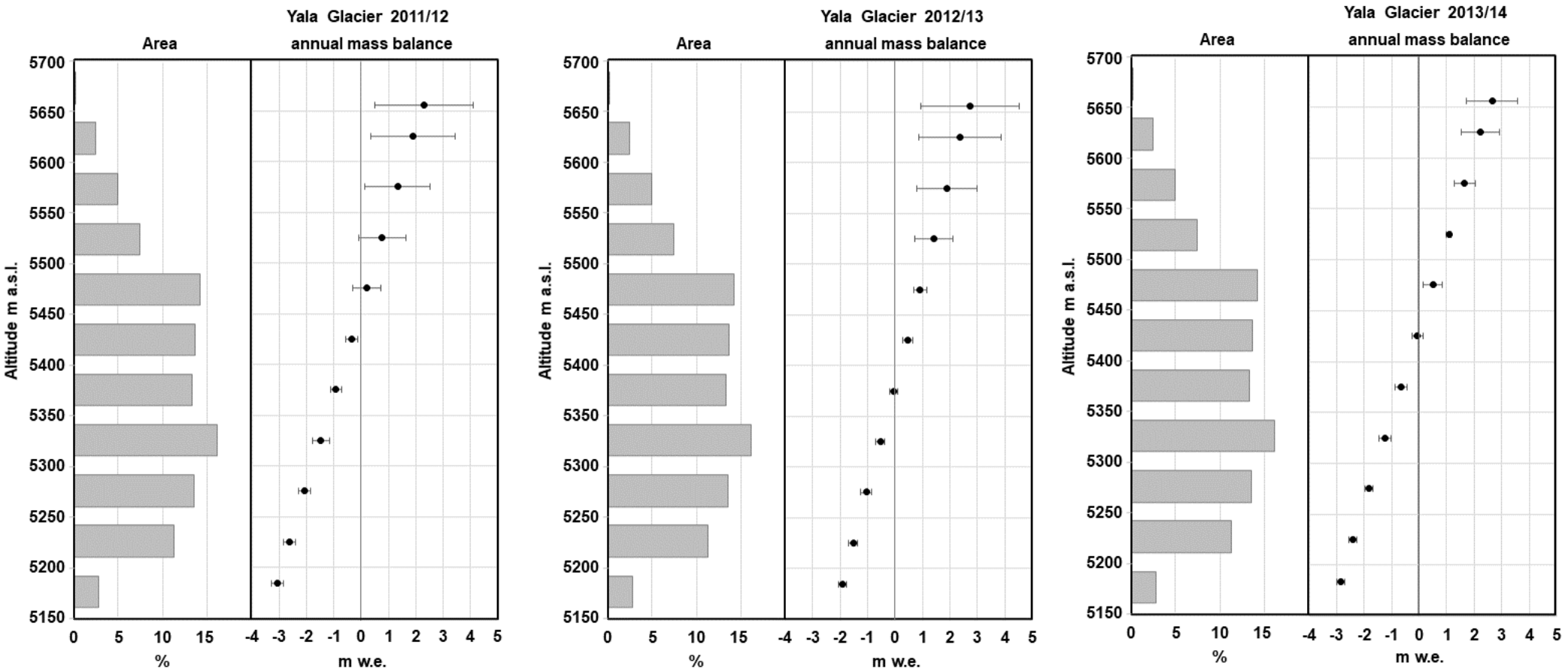

Figure S3: The annual mass balances and uncertainties for 50 m elevation bands of Yala Glacier for the mass-balance years 2011/12, 2012/13 and 2013/14. Please note, for the FoG database, the uncertainty is submitted as single value valid for the positive and negative uncertainty.

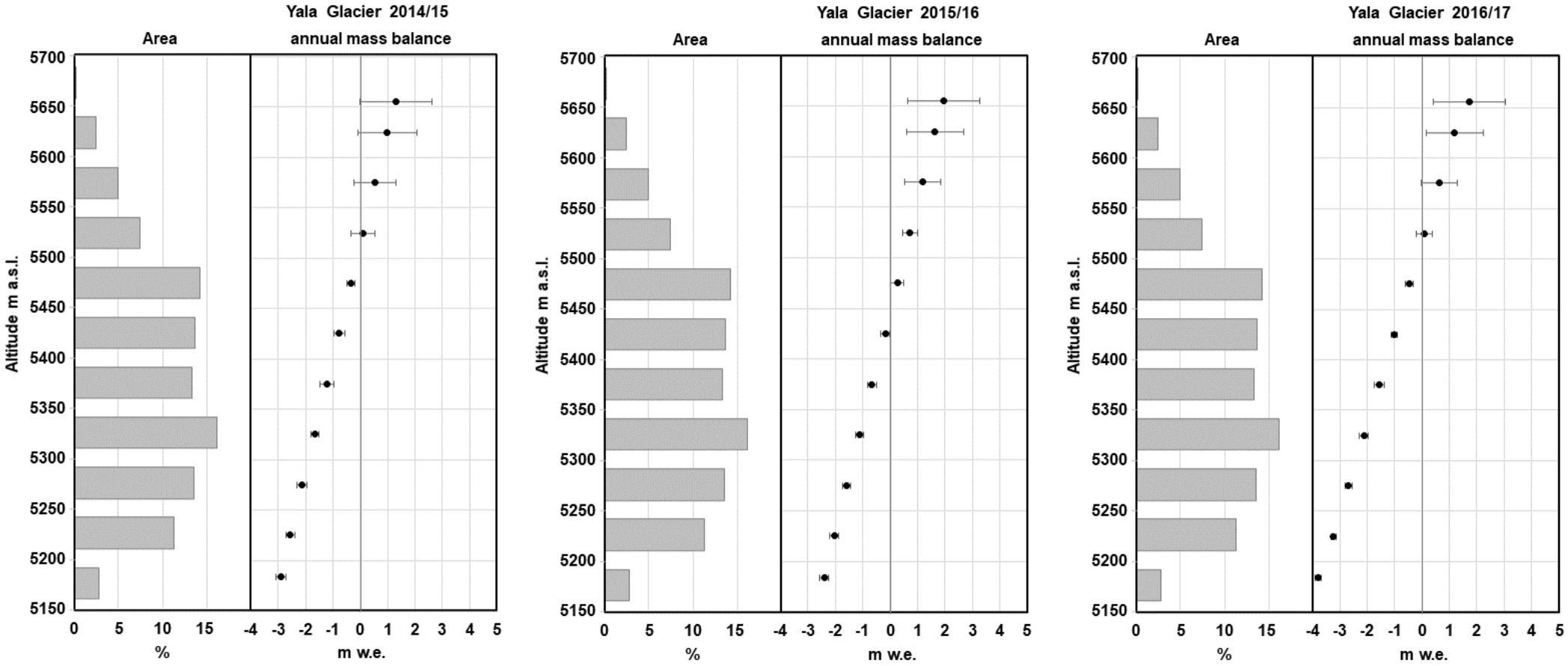

Figure S4: The annual mass balances and uncertainties for 50 m elevation bands of Yala Glacier for the mass-balance years 2014/15, 2015/16 and 2016/17. Please note, for the FoG database, the uncertainty is submitted as single value valid for the positive and negative uncertainty.

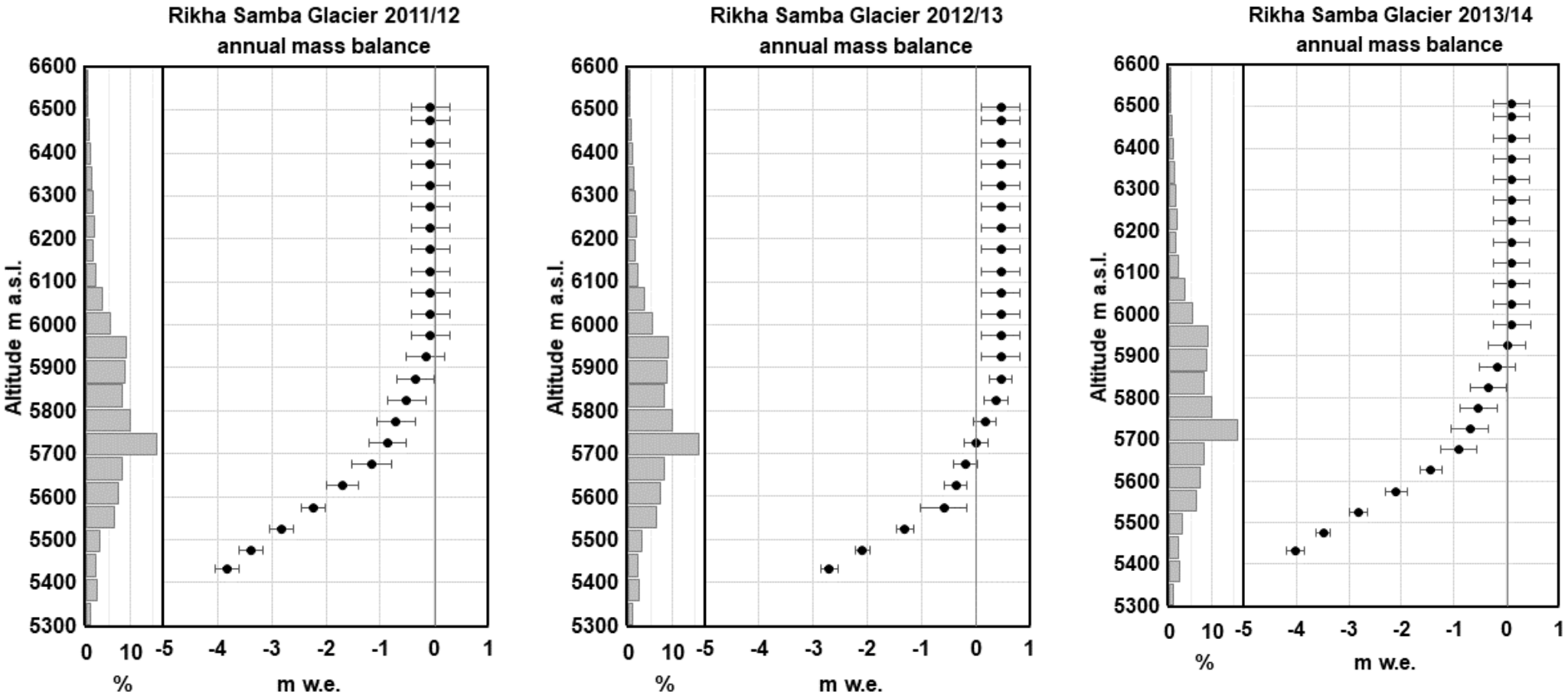

Figure S5: The annual mass balances and uncertainties for 50 m elevation bands of Rikha Samba Glacier for the mass-balance years 2011/12, 2012/13 and 2013/14.

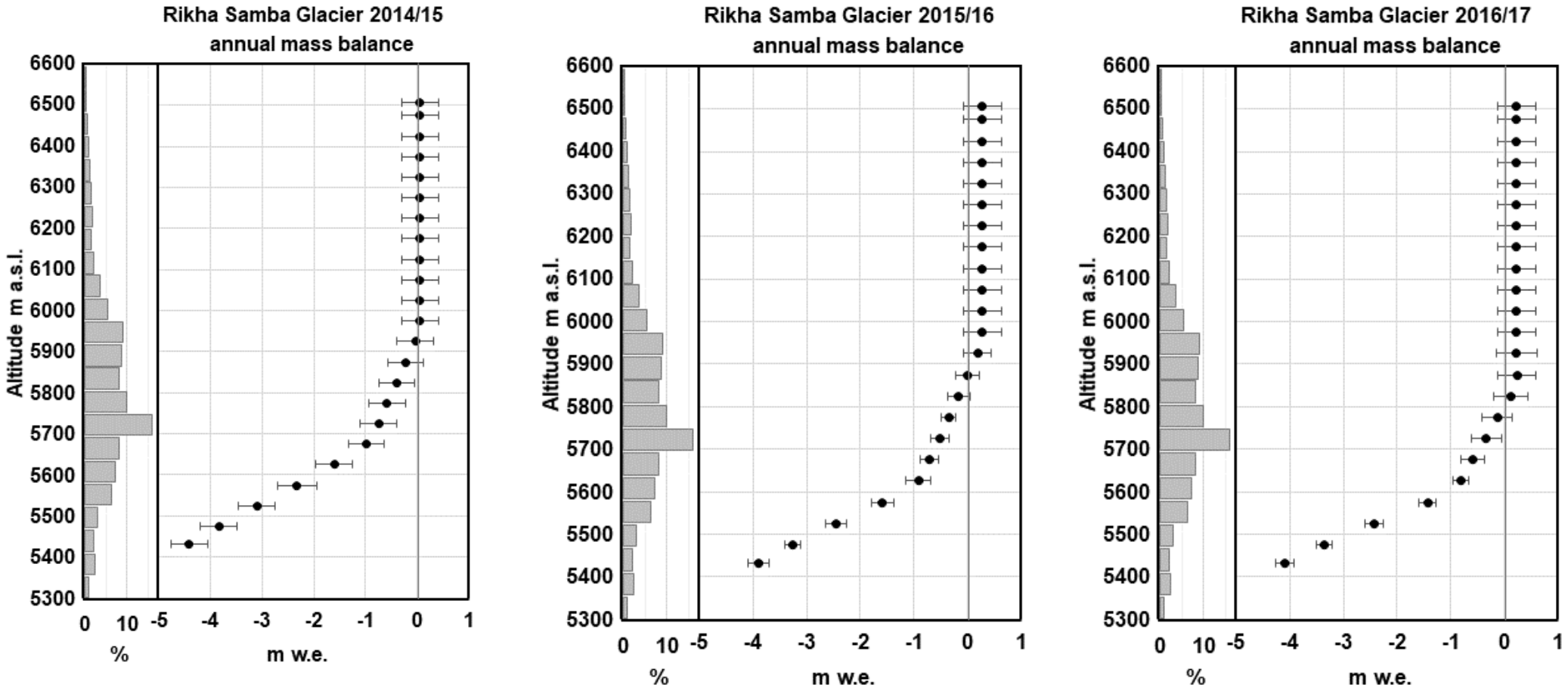

Figure S6: The annual mass balances and uncertainties for 50 m elevation bands of Rikha Samba Glacier for the mass-balance years 2014/15, 2015/16 and 2016/17.

S4 The representation of the surface area, angle and height of slopes in DEMs of various resolutions

In digital elevation models (DEM) the surface area of steep slopes is underrepresented (Fig. S7), and vertical or near vertical ice cliffs cannot be represented in a DEM at all. The steeper the slopes, the smaller is the surface area in a DEM, in particular for DEMs with a coarse resolution.

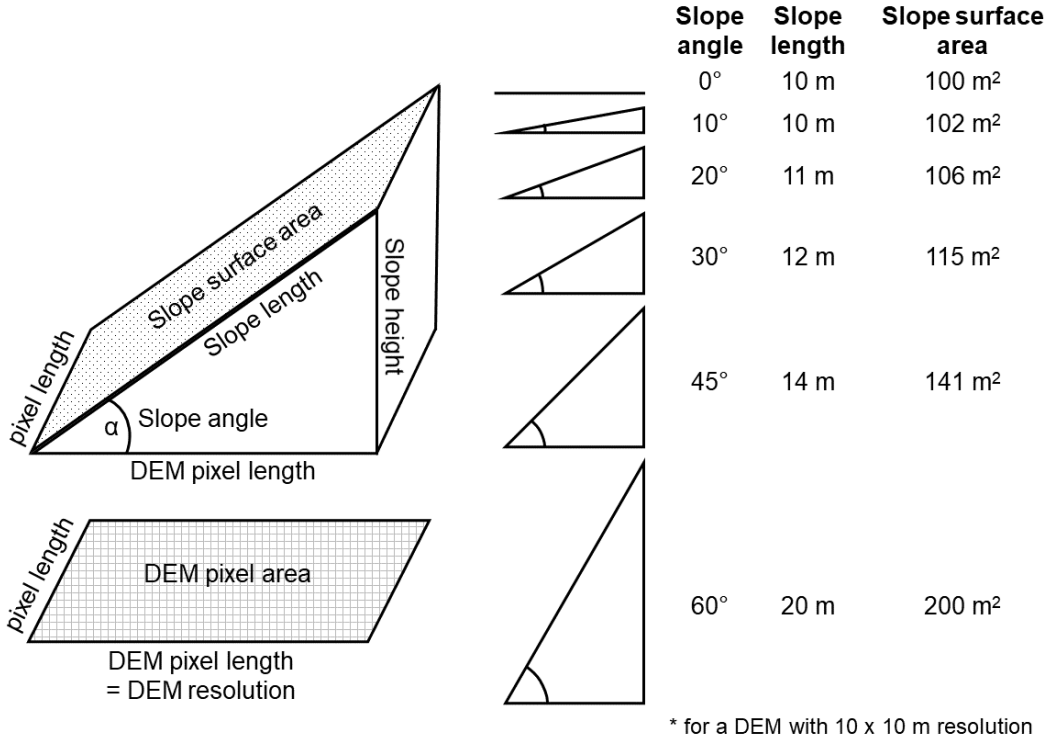

Figure S7: With an increasing slope angle the slope surface area and length increases, while the represented area in a DEM remains the same. Schema with terms (left) and examples of slopes and corresponding slope lengths and slope surface areas based on a DEM with a resolution of 10 m (right).

High resolution DEMs can represent small as well as big slope angles and slopes heights (Table S4 and S5, Figure S8). DEMs with a coarse resolution can only represent slopes with smaller angles and bigger heights.

Table S4: Minimum slope heights for various DEM resolutions (5 m, 10 m, 30 m and 90 m) that can be represented for specific slope angles.

	Minimum slope height (m) for:			
Slope angle	DEM resolution 5 m	DEM resolution 10 m	DEM resolution 30 m	DEM resolution 90 m
0°:	0	0	0	0
10°:	1	2	5	16
20°:	2	4	11	33
30°:	3	6	17	52
40°:	4	8	25	76
45°:	5	10	30	90
50°:	6	12	36	107
60°:	9	17	52	156
70°:	14	27	82	247
80°:	28	57	170	510
85°:	57	114	343	1029
89°:	286	573	1719	5156

Table S5: Maximum slope angle that can be represented in a DEM with a given resolution for a minimum slope height.

	Maximum slope angle for:			
Slope height	DEM resolution 5 m	DEM resolution 10 m	DEM resolution 30 m	DEM resolution 90 m
5 m:	45°	27°	10°	3°
10 m:	63°	45°	18°	6°
20 m:	76°	63°	34°	13°
30 m:	81°	72°	45°	18°
50 m:	83°	79°	59°	29°
100 m:	87°	84°	73°	48°

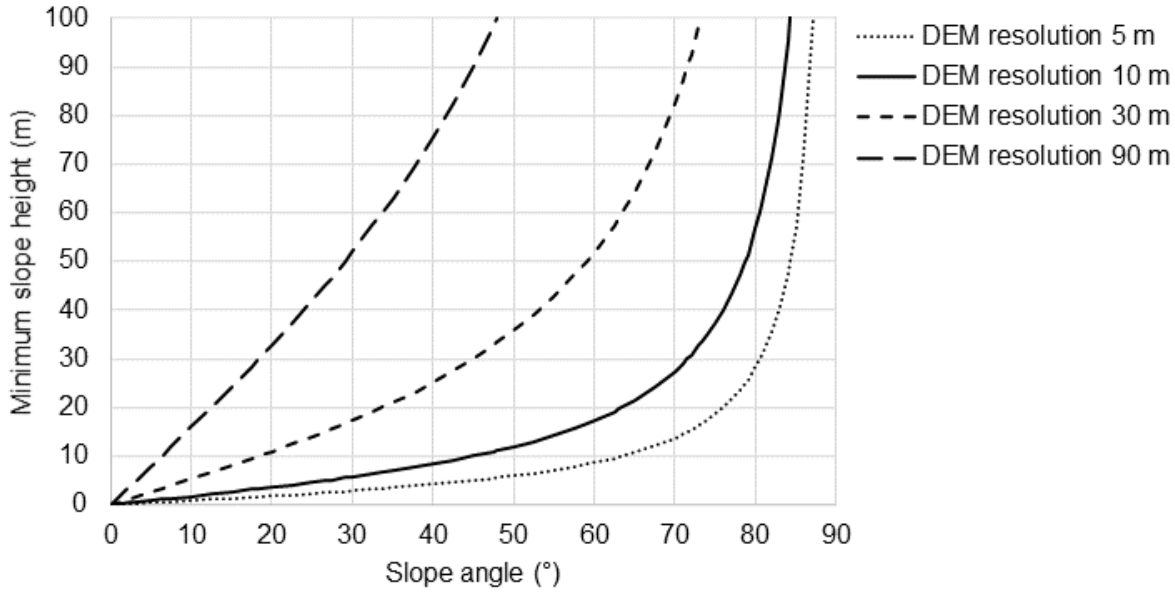

Figure S8: The curves show the minimum slope height required to represent slopes of a given angle in DEMs with a resolution of 5 m, 10 m, 30 m and 90 m.

The slope surface areas of flat slopes are better represented in a DEM than the surfaces areas of steep slopes (Table S6). For example, in a DEM with a resolution of 10 m one pixel has an area of 100 m^2. A slope of 10° has a surface area of 102 m^2 and a slope with an angle of 60° has an area of 200 m^2, which is almost double the area. Slopes of 76° and 83° have a surface area of 400 m^2 and 800 m^2, respectively. The higher the resolution of a DEM, the better is the slope surface area represented also for steeper slopes (Fig S9).

Table S6: The surface area of slopes with varying angles and the respective related height change for a DEM with a resolution of 10 m.

Slope angle (°)	Slope length (m)	Slope surface area (m^2)	Area in DEM (m^2)	Area gain* (surface vs map view) (%)	Height change (m)
0	10	100	100	0	0
10	10	102	100	2	2
20	11	106	100	6	4
30	12	115	100	15	6
40	13	131	100	31	8
45	14	141	100	41	10
50	16	156	100	56	12
60	20	200	100	100	17
70	29	292	100	192	27
80	58	576	100	476	57
85	115	1,147	100	1047	114

* surface gain irrespective of DEM resolution

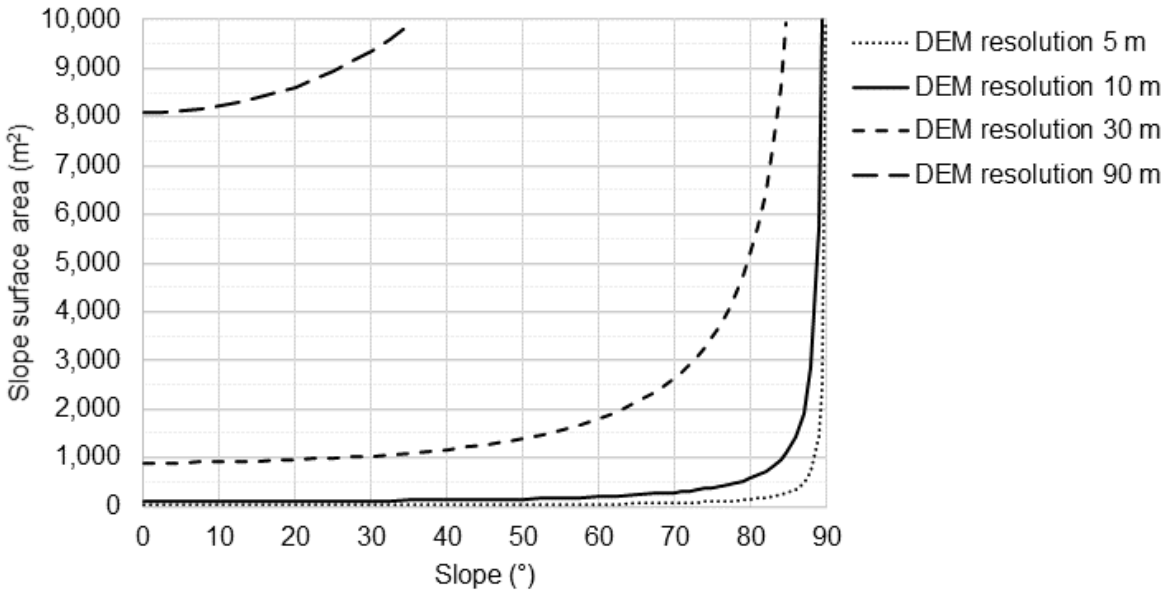

Figure S9: The slope surface area increases with increasing slope angle at different rates for DEMs with resolutions of 5 m, 10 m, 30 m and 90 m.

S5 References

Ageta, Y. and Higuchi, K.: Estimation of Mass Balance Components of a Summer-Accumulation Type Glacier in the Nepal Himalaya, Geogr. Ann. Ser. A Phys. Geogr., 66, 249–255, https://doi.org/10.1080/04353676.1984.11880113, 1984.

Fujita, K., Sakai, A., and Chhetri, R. B.: Meteorological observation in Langtang Valley, Nepal Himalayas, 1996, Bull. Glaciol. Res., 15, 71–78, 1997.

Kaser, G., Fountain, A., and Jansson, P.: A manual for monitoring the mass balance of mountain glaciers. Technical Report 59, International Hydrological Programme. IHP-VI. UNESCO, Technical Documents in Hydrology, 2003.